Preprint YERPHI 1445(15)-95

ԵՐԵՎԱՆԻ ՖԻԶԻԿԱՅԻ ԻՆՍՏԻՏՈՒՏ
ЕРЕВАНСКИЙ ФИЗИЧЕСКИЙ ИНСТИТУТ
YEREVAN PHYSICS INSTITUTE

Shikhliarov, V.G.Gavalian, M.A.Aginian

DETECTING PART OF TRD FOR GINES INSTALLATION

Ереван

NOTICE

PLEASE BE AWARE THAT THIS IS THE BEST REPRODUCTION POSSIBLE BASED UPON THE ORIGINAL DOCUMENT RECEIVED

Published
NIM-A371, 406-413, 1996

1. Introduction

In recent years there appeared huge transition radiation detector (TRD) projects. A good example is the integrated TRD project on LHC [1]. In certain stages of realization are the neutrino project with fixed-target WA96(NOMAD) [2] on SPS and GINES (hybrid neutrino spectrometer) on UNK [3]. In both projects the working area of TRDs is $\sim 10 m^2$. With such large dimensions, there arise certain problems with the radiators as well as X-ray transition radiation (XTR) detectors. Increasing dimensions of the installations and almost 4π geometry of the experiments on colliders increase the probability of using irregular radiators in spite of their somewhat lower (from 10 to 20%) radiating power. The latter circumstance, however, has stimulated us to search for non-standard solutions for construction of just a strictly regular radiator with a large efficient area. In result, we have constructed a new radiator which we named pneumatic radiator of secondary radiation, the description of which will be given elsewhere.

In this paper we present the results of some investigations on XTR detectors, carried out in the framework of GINES (UNK) collaboration for large-size TRDs.

2.General Description of TR Detectors

2.1 Selection of TR Detector Type

In case of large TRDs, the use of multiwire detectors is not optimal. That is why we decided to incorporate in TRDs detecting surfaces in the form of aluminized mylar straws with diameter 16mm. Such a choice solves several problems:

1. The specific problem at XTR detection, connected with the hydrostatic pressure on the windows, which is due to the use of the heavy gas xenon, is absent.

2. The thin walls are easily penetrated by low-energy quanta and cause no multiple scattering.

3. The corona discharge or breakage of the wire create problems of a local character.

4. Possibility for quick changing of the straws.

5. The closed cathode provides for a good electric decoupling.

6. The possibility of having higher pressure, which on the one hand, off-loads the carrying constructions and, on the other hand provides for a higher coordinate accuracy.

7. Flexibility to the geometry of experiment.

2.2. Optimal Number of Straw Rows in a TRD Module.

To find the optimal number of straw rows in one TRD module, we carried out a Monte Carlo calculation of two TRD versions using the maximum likelyhood method, in which the total number of straw rows and the total number of layers in the radiators was the same. The first version contained 12 radiators each with 250 polypropylene films and 12 doubled rows of straws. The second version contained 24 radiators each with 125 films and 24 single rows of straws. The particles direction was normal to the surface of detecting straw rows at x=5mm and x=8mm (Fig.1). The point of x=8mm is a checking point, as the results from the two versions will coincide in it within the statistical errors. In the simulation we used 10^6 electrons with E_e=4GeV and 10^6 pions. As is seen from Fig.2, at x=8mm the results coincide, but at x=5mm, for the second version the rejection is improved by an order of magnitude.

2.3. Straw Manufacturing and Fastening Technique

A simple technique of manufacturing of straws from aluminized mylar strips has been devised. We made 3m long samples with diameter 16mm and walls thickness 12um. The straws are made of 5cm-wide mylar strips, the edges of which are applied with non-drying glue. The strip is wrapped around a gauge tube of 16mm diameter. While wrapping, the straw is periodically removed from the gauge. Then an overpressure of P=2atm is applied to the straw, the testing and strengthening of the glue line taking place simultaneously. Straws with walls of 12mm thickness withstand ~2.5atm of overpressure. The ready straws are perfect and light (~10g) cylinders. The ends are stretched on the end-piece with 16mm diameter, made of the same gauge as

the gauge tube, this providing a tight fit of mylar straws without their deformation.

A signal wire of diameter 100μm is stretched through the centers of the end-pieces and the straw. Use of thick wire allows to assemble straw rows by soldering the wires to the strips on the fiberglass frame, like in usual multiwire proportional chambers. Such construction provides for a gapless tight straws packing and an easy changing. To test our decisions, we constructed a 12-module working TRD with an aperture of $(20\times26)cm^2$ and a length of 120cm (Fig.3).

2.4. Mode of XTR Detection

A method of XTR detection in the self-quenching streamer mode was proposed in the papers [4-6]. The essence of the method is in the fact, that at a certain supply voltage, the ionization distributed along the particle's path initiates proportional avalanches near the wire, and charge clusters formed by XTR quanta and δ-electrons create avalanches, turning nonlinearly into a streamer which induces a signal tens of times surpassing the amplitude in the proportional region. The nice side of this mode is that the clusters are selected not by an external electronic device, but by the wire itself. The main advantages of the mode in the working point of TRD are: high signal amplitude, exceptional noise immunity, practical lack of noises, threshold-independence in a wide range, possibility of signal transmission to large distances without preamplification. Rate capability of the mode is $\sim10^6c^{-1}$ per meter of wire, this meeting the requirements of neutrino experiments. One can speak about only a conditional cluster counting technique, as no more than one cluster is registered on the path of particle in the streamer mode ("Yes"-"No" mode). If the average number of clusters from a light particle is comparable with that of the TRD modules, then the frequency of responses from the modules will have a binomial distribution. But if the number of modules is about twice as the average number of clusters, then we have a Poisson distribution and can speak about a cluster counting technique.

3. Laboratory Testing of Straws

3.1. Preliminary Considerations

Though the self-quenching streamer (SQS) mode and the detectors constructed on its basis are intensely investigated in the last 15 years, nevertheless they have a definite trend - construction of reliable coordinate detectors. We are interested in this mode from the viewpoint of XTR detection on the background of the ionization distributed along the particles path. This predetermines, on the one hand the use of the heavy gas xenon and its studying in the SQS mode, which has not been carried out in virtue of a different trend of investigations, and on the other hand - revealing certain features not usually manifesting themselves in the SQS mode.

In the 3m-long straws, aside from the strength tests, we studied the gas gain factor (GGF) along the signal wire. The measurements showed stable signal height spectra on the length of 3 meters. The other investigations were carried out on 20cm-long straws. In the laboratory investigations we used ^{55}Fe, ^{241}Am, ^{90}Sr radioactive sources. Gas mixtures of $Xe+CH_4+He+C_3H_8O_2$ (methylal vapours) and $Xe+CH_4$ of different concentrations were used as gaseous filling agents.

3.2. Streamer Signal Height to Cluster Charge Correlation

In our paper [5] we have shown that the streamer peaks, obtained at the wire's exposure to electrons from ^{90}Sr and γ-quanta from ^{55}Fe are shifted from each other (Fig.4). To explain it, we may assume that in the gaseous mixture containing effective quenching admixtures (methylal) there takes place a partial correlation between the streamer signal height and the energy (charge) of the cluster having produced the streamer. To clear up this question, we have calculated the W(E) spectrum of clusters registered in SQS mode and formed on the minimum ionizing electrons path, provided the probability of transformation into a streamer for a quantum with E_γ=5.9keV, which we will call a reference one, is 80%. For simplicity, it is assumed that the clusters spectrum has a Rutherford distribution P(E), and the probability $W_{str}(E)$ of transformation into a streamer for a cluster with energy E has been calculated by

Raether's data [7]. Then $W(E)=P(E)W_{str}(E)$. These three dependences are shown in Fig.5, where it is seen, that the poorly expressed maximum of W(E) falls on ~2keV, and more than half of the registered clusters have an energy of <5keV. Thus, the shift of the spectra shown in Fig.4 becomes clear, if assumed there is a partial correlation between the signal height and the cluster's charge and the form of the spectrum of W(E) is taken into account. For the same reason, a spectrum shift is observed in the presence of methylal vapours and at exposure of the straws to different γ-sources. Fig.6 shows the spectrum shift for the γ-quanta from ^{55}Fe and ^{241}Am. Thus, it is possible to improve the particle rejection by measuring both the number and the charge of streamers. In the absence of methylal vapours the charge-amplitude correlation vanishes. Though the methylal admixture stabilizes the detector's performance and provides some possibilities in the plane of the effects described, its utilization is not convenient. We carried out a series of investigations of gaseous mixtures not containing methylal vapours.

3.3. Cluster Detection Threshold

The avalanche-to-streamer transformation is of a statistical character. In principle, all the keV clusters can initiate a streamer, but, as is seen from Fig.5, with different probability. So, the notion of cluster registration threshold in this case is unclear and, as distinct from the proportional mode, has nothing to do with the electronic threshold, which can be set in a wide range. However, the situation clears up, if the probability of transformation into streamer for the clusters with reference energy of E_γ=5.9keV (^{55}Fe) is given.

3.4. Efficiency of Minimum Ionizing Particle Detection by Clusters

The problem of δ-cluster background, arising in the gas as a consequence of particle transit, becomes important, as it affects the particle separation efficiency. That is why, already under laboratory conditions it is desirable to measure the efficiency of detection of the particle not accompanied by

transition radiation, in dependence with Xe concentration and probability of transformation into streamer of a cluster with reference energy. For this purpose, the electrons at the end of the spectrum of ^{90}Sr (E_{max}=2.2MeV) have been used as incident particles. The efficiency of their detection has been determined by the ratio of the number of responses of the straws in the streamer mode to the total number of electrons having traversed it. At the same time we measured the efficiency of detection of the clusters with reference energy of E_γ=5.9keV. The measurements were carried out in dependence with the voltage applied to the straws. Compilation of the results obtained allows us to plot the dependence shown in Fig.7a for the gaseous mixture of $Xe+CH_4+He+C_3H_8O_2$ and in Fig.7b for $Xe+CH_4$.

The efficiency W_{cl} of the minimum ionizing particles detection by δ-clusters with $E_\delta \geq 1$keV produced in the gas, is laid as the ordinate axis. Each curve corresponds to a definite probability of transformation into streamer for a reference cluster with E=5.9keV. This statement can be interpreted otherwise, namely, to each curve corresponds a definite efficiency of detection of an XTR quantum with energy E_γ=5.9keV. In, e.g., Fig.7a, at W_{cl}=8% and 40% Xe concentration the efficiency of detection of ~6keV XTR is 80%, the quanta with E_γ<6keV being registered in accordance with the curve 2 shown in Fig.5, while those with E_γ>6keV - with an efficiency of >80%. For comparison, in Fig.7a are presented the efficiency of detection of ^{241}Am quanta (E_γ=13.8keV and higher), averaged over all the γ-lines. It is seen that the probability of transformation into streamer for ^{241}Am is higher than for ^{55}Fe, this difference decreasing with increasing W_{str} (with increasing supply voltage). The measured and the calculated δ-cluster backgrounds are in a good agreement. The integral on the W(E) curve in Fig.5 is ~0.18, this corresponding to the electron detection efficiency (Fig.7b) on the curve of W_{str}=80% at 80% Xe concentration (1cm Xe). The data of Fig.7 are used in the TRD optimization and particle rejection calculations.

3.5. The Probability of Transition into Streamer as a Function of Location of Straw's Bombardment

The presented values of the probability of transformation of reference clusters into streamer are obtained at integral irradiation of the straws. However, it can be assumed that as a result of the charge drift and diffusion, its density decreases, which can affect the probability of transition into streamer. To check this, the straws were exposed to a pencil (500μm) beam of reference quanta in three points. The corresponding counting characteristics are presented in Fig.8. It is seen that at U=3.1kV, when the drift is relatively slow, the ratio of the probabilities of transition into streamer for the extreme curves is ~3, while at U=3.2kV this ratio is close to unity. Hence, the integral value of W_{str} at working voltages describes the straws operation well, regardless the location of quantum absorption.

It is interesting to note that in a usual proportional drift chamber the charge diffusion leads to an opposite result, i.e. the signal height from the charge close to the signal wire proves to be lower than that from the charge drifting from a farther distance [8].

3.6. Gas Gain Factor

To determine the gas gain factor (GGF), we measured the average current I from an irradiated straw as a function of the supply voltage U. This method, as apposed to the CDC method, allows one to consider in details the peculiarities of the process. In this case GGF can be defined as:

$$GGF(u) = \frac{6.2 \cdot I(nA) \cdot W_1(eV)}{N_{pl} \cdot \Delta E(eV)} \qquad (1)$$

where N_{pl} is the number of particles having traversed the straw, or the number of γ-quanta being absorbed in the gas in unit time, w_1 is the energy consumed to form an electron-ion pair, ΔE is the total energy deposited by a particle or a quantum in the gas.

Fig.9 shows GGF as a function of U for the gaseous mixture of 40%Xe+60%CH_4 (curve 1). To analyze this curve, in this fi-

gure is presented also the counting characteristics of the 40%Xe concentration (curve 2). It is seen from curve 2, that the streamer formation starts from U≥3100V. Consequently, curve 1 contains no streamers at U=3100V. In curve 1, the region of up to U=2800V, where GGF reaches up to $2 \cdot 10^4$, corresponds to the region of proportional gain. Then in the region from U=2800V to U=3100V the GGF increases slowlier, reaching $\sim 10^5$, i.e. still increases about 5 times. This is the limited proportionality region.

Beginning from U=3100V, the avalanche can reach a critical value and transform into a streamer. That is why in the interval from 3100V up to 3250V, in curve 2 there is observed a sharp increase of the detection efficiency, and a sharp increase in the GGF in curve 1. This region is characterized by the fact, that there are two types of signals at the same time: limited-proportional and streamer signals, the first being easily "pumped" into the other.

Curve 2 has a knee in the interval from 3200V to 3300V, where 10% of the remaining proportional signals turn into a streamer, but this does not practically affect the GGF. That is why at U≥3250V GGF increases only in the streamer mode.

For comparison, in Fig.9 the curve 3 for the gaseous mixture of 42%Xe+28%CH_4+30%$C_3H_8O_2$ is also presented. It is hard to explain unambiguously the small but stable increase in the GGF for this mixture in the proportional region. This possibly results from a slight difference in the Xe contents. Another explanation is the charge gain due to electron impact at the expense of the low methylal molecules ionization potential (I=9.98eV) and the large cross section of this process. The comparison of curves 1 and 3 allows one to understand the role of methylal in different stages of streamer formation. It is seen that methylal vapours do not affect the beginning of the streamer formation process, which in either cases starts at GGF≃10^5. The same is true for the rate of transformation into streamer. On the other hand, the presence of methylal vapours contributes to a considerable (in this case 7 times) suppression of the signal height. Thus, one can conclude that methylal, due to the large cross section of photoabsorption, plays

an essential role only in the stage of streamer growth , but never in the processes of avalanche formation and their reaching a critical size and transformation into a streamer.

It is seen in Fig.9 that the avalanches reach a critical value at $GGF \simeq 10^5$ or at the critical number of particles in them $n_e \simeq 2.7 \cdot 10^7$. At the same time, according to Raether's data [7], the beginning of streamer formation in a uniform field corresponds to $n_e \geq 2 \cdot 10^8$, which exceeds the our obtained value by an order of magnitude. We suppose that this difference is due to the very strong field near the wire ($\sim 10^5$ V/cm).

3.7. Time Spectra, Drift Time and Drift Velocity

The straw's time spectrum has been measured in a gaseous mixture of $Xe+CH_4$ in a wide Xe concentration variation range. The straw was exposed to ^{90}Sr electrons at the spectrum edge. Fig.10 shows the total drift time as a function of Xe concentration. An analogous dependence for the drift velocity is also presented in the same figure. The measurements were carried out at two supply voltages: on the plateau, and when 80% of reference clusters passed into a streamer, no changes being observed in the spectrum. Fig.11 shows the time spectra in case of 50% Xe concentration. Straws were bombarded at angles $\theta=0$ and 20^o to the normal to its axis. The unusual shape of the spectrum is attracting, which requires an explanation. As straws operate not only in the SQS mode, but also in the mode of registration of keV clusters, then there is measured not the time of the arrival of the nearest electron, but the drift time of the δ-cluster, which can be produced equiprobably in any point of the track. As far as the number of δ clusters Δn is proportional to the surface ΔS of a ring with width Δr, and $\Delta S \sim r$, then the number of δ-clusters $\Delta n \sim r$. Hence, at a uniform bombardment of straws, each point of the time spectrum is set up as a result of the clusters drift from the isochrone of the radius r. Then the r(t) function will be expressed as :

$$r(t) = \frac{R}{N_o^{1/2}} \left\{ \int_o^t \frac{dN}{dt}\, dt \right\}^{1/2} \qquad (2)$$

where R is straw's radius, N_o is the area under the spectrum.

To have the shape of the spectrum in more details at short times, we carried out measurements with a flat electron beam with a width of 2mm and an angular spread of $\sim 7^{o}$, incident on the centre of a vertically installed straw ($\theta=0^{o}$), i.e. we selected the electrons passing near the signal wire at a distance of $\Delta 1 \leq \pm 1$mm and angle $\theta=0$ in the angular range of $\Delta\theta \leq \pm 3.5^{o}$. The corresponding time spectrum is shown in Fig.12, where the frequency of the events from the particles incident almost vertically on the wire dominate in the interval of short times. At a straw's inclination of $\theta=20^{o}$, this effect is weaker (Fig.12). Finally, at $\theta=20^{o}$ and additional collimation over θ within $\Delta\theta \leq \pm 0.5^{o}$, the effect vanishes. In this case the drift time distribution corresponds to the expected one. So, one can conclude that for particles incident radially on the wire, the probability of short times increases. The most likely explanation of this effect is in the total influence of small clusters that drift to one point, the more so that Xe has an abnormally high total-to-primary-ionization ratio [9]. It is interesting to note that still in 1947, in [10], where the shape of the pulses in the proportional chambers with a high vapour contents was studied, there were observed so-called enlarged pulses at a radial bombardment with both α and β particles. These enlarged pulses belonged to neither the proportional nor the Geiger modes. Now we can make a statement, that already in the late 40-ies some authors observed the SQS mode, but, unfortunately, attached no methodical importance to it. It was only noticed, that the effect was of great importance for studying the gas discharge physics [11].

3.8. "Dead" Zone and Rate Capability

Though the rate capability in the SQS mode has been more than once measured [12,13], there are no corresponding data for the mixture of $Xe+CH_4$. To determine the maximum rate capability, we measured the "dead" zone on the wire in the place of streamer formation. For that purpose we used, we think, the most suitable method of self-coincidence suggested in [12]. A certain length of the straw was exposed to quanta with energy E_γ=5.9keV at a supply voltage at which 80% of reference clusters are transformed into a streamer. The measurements were

carried out in a wide range of Xe concentrations. Fig.13 shows the measured "dead" length as a function of time, for certain Xe concentrations. The integral over the curve determines the "dead" zone ξ. Fig.14 shows the "dead" zone ξ as a function of Xe concentration. To estimate the rate capability, let us consider, e.g., the dead zone of ξ=122μs·cm at 50% Xe concentration. The maximum load is defined as $\xi^{-1}=8.2\cdot10^{3}cm^{-1}s^{-1}$. So, the maximum load per TRD module with sizes $3x3m^{2}$ and straw diameter 16mm will be $\sim5\cdot10^{8}s^{-1}$, the loading being by reference quanta. As to loading by particles, remember (Fig.7b), that at a 50% Xe concentration and W_{str}=80%, the particle detection efficiency is ~0.12. So, the expected maximum load can be estimated as $\sim5\cdot10^{9}s^{-1}$ per TRD or $\sim5\cdot10^{8}s^{-1}m^{-2}$.

3.9. Noises

The level of noises in the our manufactured 20cm-long straws of 12μm-thick mylar film with a 260Å aluminum coating and a signal wire with 100μm diameter is extremely low. The number of noise pulses, including the cosmic background, at working voltages was no more than $n\simeq2s^{-1}$, regardless Xe concentration. Another straw with a ~60Å aluminum coating behaved quite differently in the sense of noises. Its noise characteristics are presented in Fig.15. The noise pulses and the dark current were measured simultaneously. At an additional illumination by a usual incandescent lamp, the number of noise pulses and the current increased. The straw with a 260Å coating did not react to the additional illumination. The effect of the daylight on the noise characteristics of proportional chambers with an aluminized mylar cathode has been noticed in [14], and in [15] this effect was studied in details and shown to be due to escaping of single electrons from the cathode, apparently in the strong electric field induced by the ions on the surface of Al_2O_3. In our case, noise was observed in the SQS mode, so we cannot accept the hypothesis of single electron, the probability of transformation of which into a streamer in the given case is equal to zero. So, this interesting problem requires a special consideration.

4. Detection of TR on Electron Beam

To clear up the question of a simultaneous detection of particles and TR in cylindrical detectors in the SQS mode, the straws filled with a gaseous mixture of 40%Xe+10%CH_4+41%He+ +9%$C_3H_8O_2$ were exposed to an electron beam in the energy range of E_e=(0.3÷2.8)GeV. The first preliminary results are presented in Fig.16 and 17. Fig.16 shows the 1.8GeV electrons detection efficiency as a function of the voltage applied to the straws. As TR radiators were used stacks of regular laminar media of polypropylene (PP) with a thickness of a=16μm and number of layers m=150, in the one stack the spacing being b=1.5mm, and in the other stack - b=400μm. There was also used polystyrene foam PS-4 with ρ=0.04g/cm^3 and PS-10 with ρ=0.1g/cm^3 and a length of 6cm.

To the measurement without a radiator corresponds the electron detection efficiency of only δ-clusters, which, as is seen from Fig.16, is independent of the electron energy. The working voltage was chosen to be U=2.6kV, at which 80% of reference quanta pass into a streamer. It is seen from Fig.16, that the radiation yield from the PP radiator with b=400μm is by about 20% higher than that from PS-4 with $\bar{b}$=410μm. To this excess, however, contributes also the higher quantum self-absorption in PS-4. Fig.17 illustrates the dependence of electron detection efficiency on their energy, with and without polypropylene radiator. The calculated results are presented in the same figure. One can see, that in the energy range of $E_e \geq$1.8GeV there is observed a good agreement with the theory, but for lower energies the experimental data lie considerably lower than the calculated ones.

5. Conclusion

There is developed the detecting part of TRDs based on thin-walled mylar straws with xenon filling, operating in the SQS mode. The maximum response time of the system at the straws's diameter 16mm and 50%xenon concentration is ~150ns. The rate capability of TRDs at 50% xenon concentration is on the level of $5\cdot10^8 m^{-2}s^{-1}$, which is quite acceptable for neutrino experiments. The exposition of the straws to a beam showed a

good agreement with the theory at $E_e \geq 1.8$GeV. At lower energies, an agreement with the theory have only the data at $E_e = 0.3$GeV. Now we carry out detailed investigations of the rejection factor uniformity over the area of TRDs based on straws.

* The work has been carried out under the financial support of the SINES UNK collaboration and by the grant 211-5291 YPI of the German Bundesministerium für Forschung und Technologie.

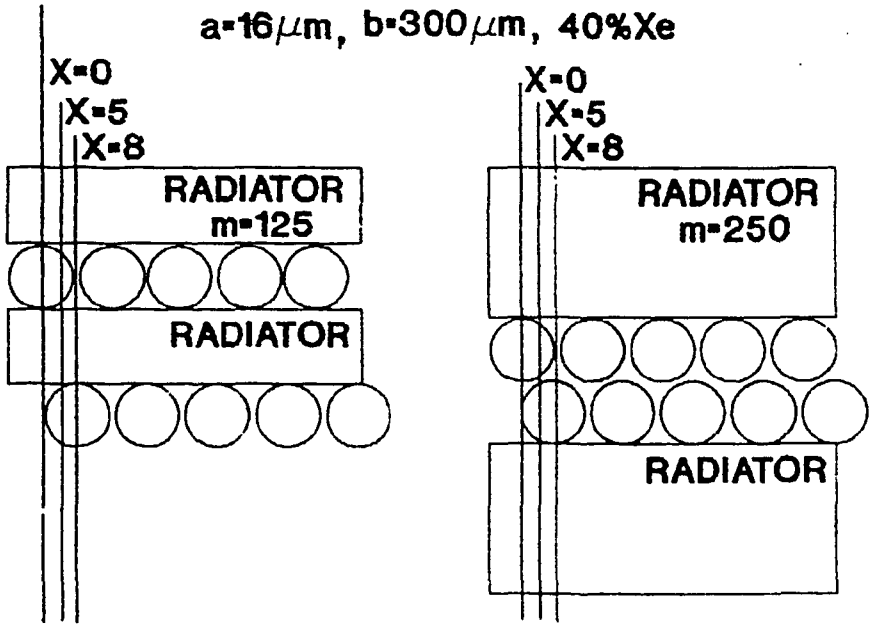

Fig.1

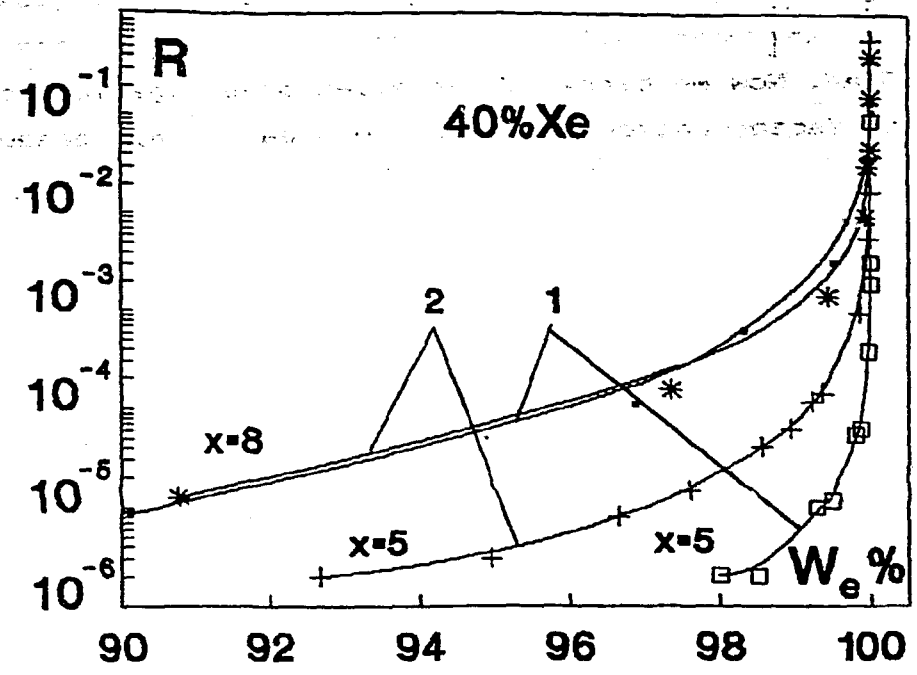

Fig.2

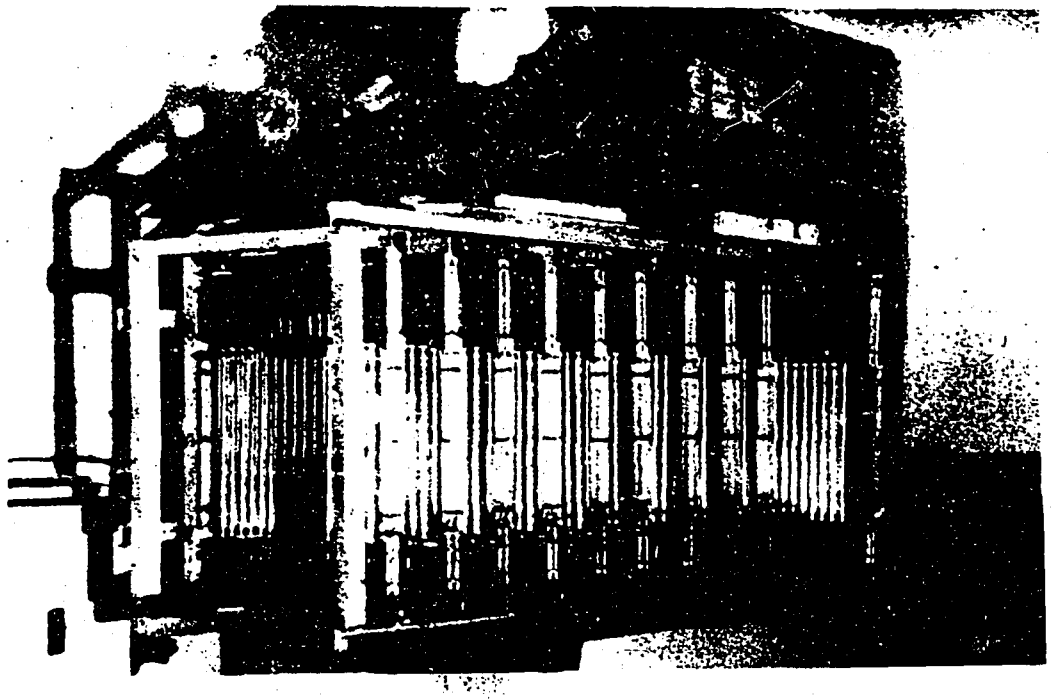

Fig.3

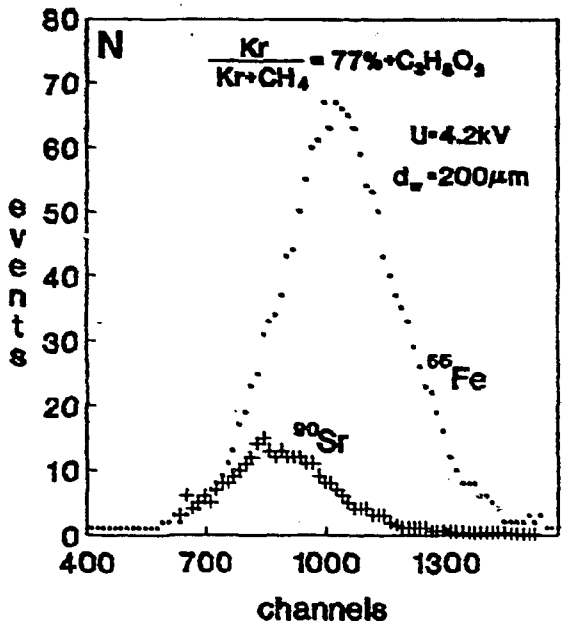
N
Kr / Kr+CH4 = 77%+C3H8O3
U=4.2kV
d=200μm
events
55Fe
90Sr
channels
Fig.4

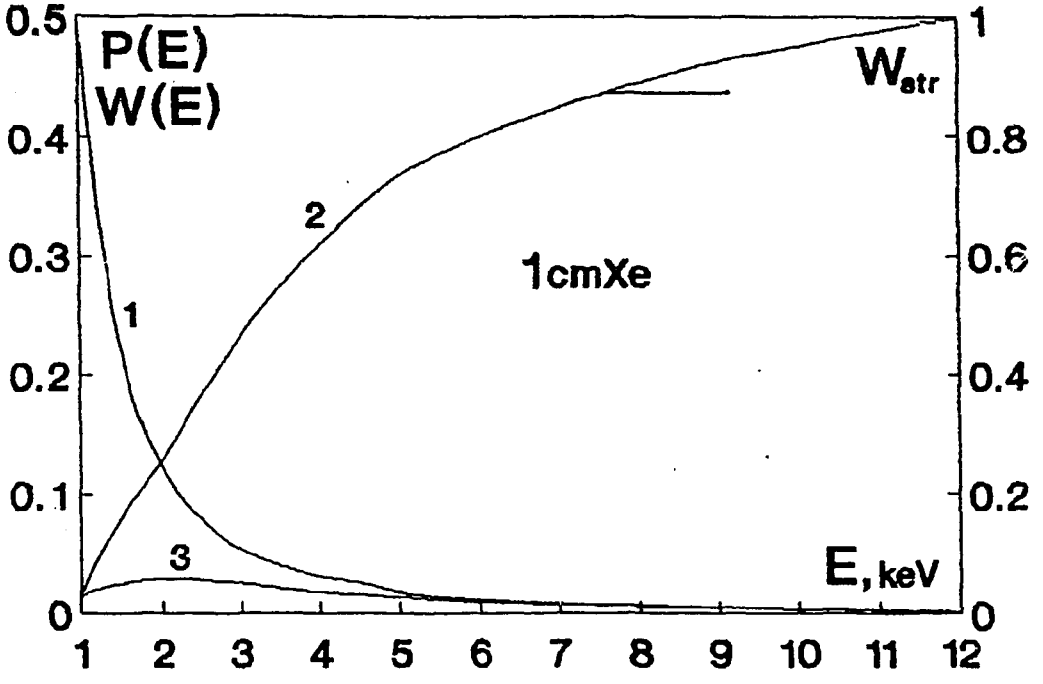
P(E)
W(E)
Wstr
1cmXe
E, keV
1
2
3
Fig.5

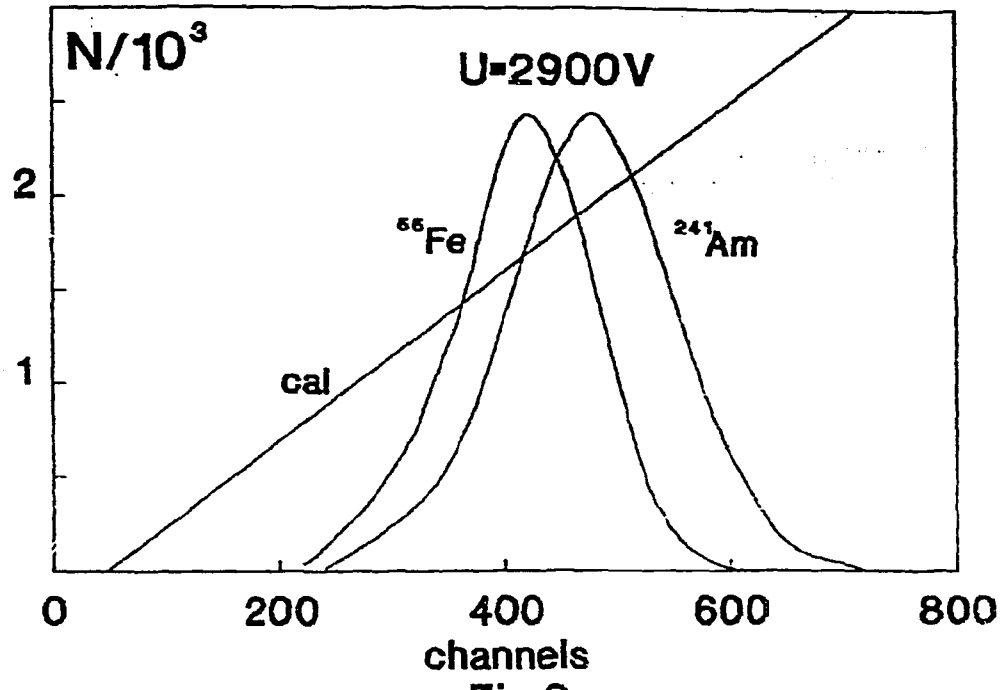
N/10³
U=2900V
2
1
⁵⁵Fe
²⁴¹Am
cal
0
200
400
600
800
channels
Fig.6

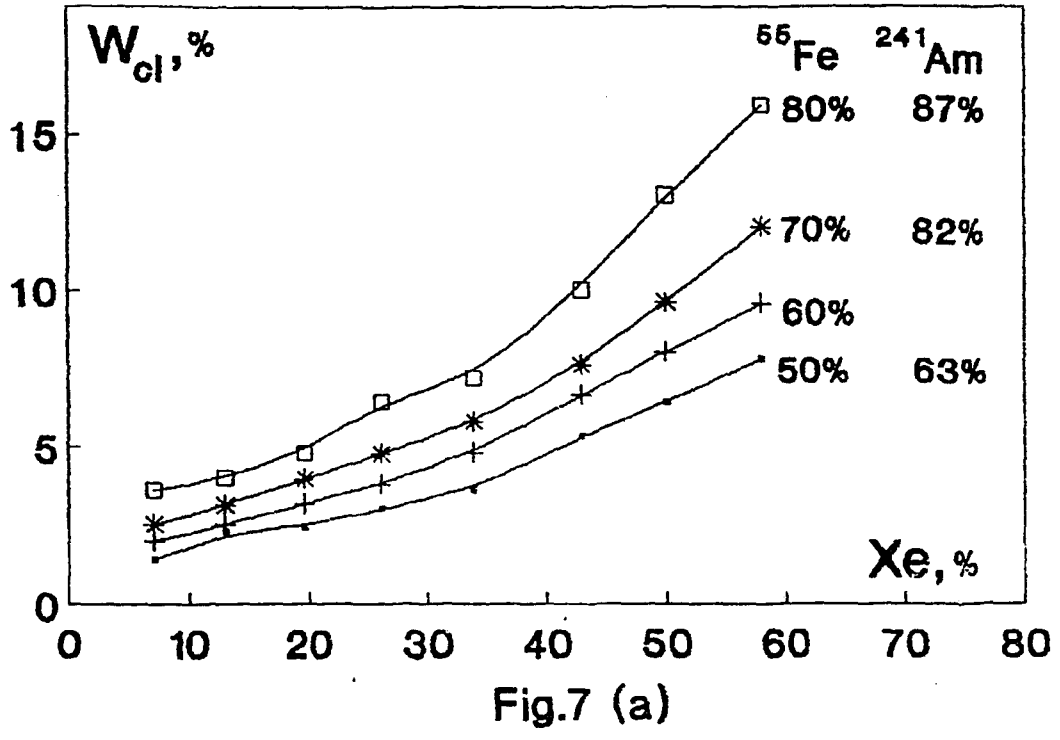
W_cl, %
⁵⁵Fe
²⁴¹Am
80%
87%
70%
82%
60%
50%
63%
Xe, %
15
10
5
0
0
10
20
30
40
50
60
70
80
Fig.7 (a)

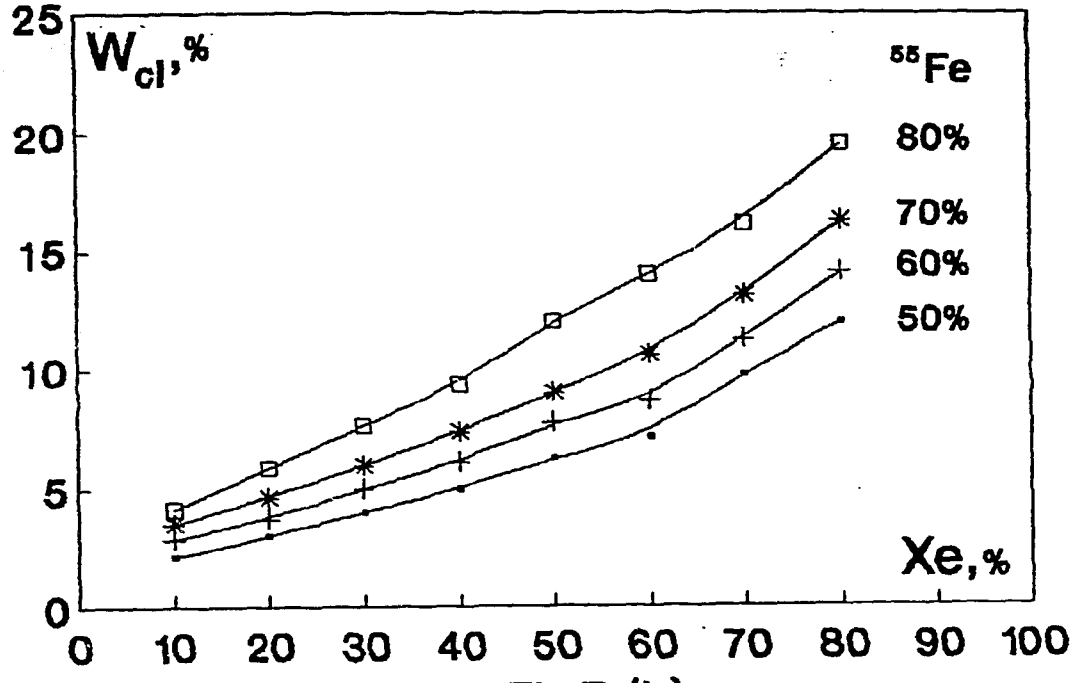
25
20
15
10
5
0
W_{cl},%
^{55}Fe
80%
70%
60%
50%
Xe,%
0
10
20
30
40
50
60
70
80
90
100

Fig.7 (b)

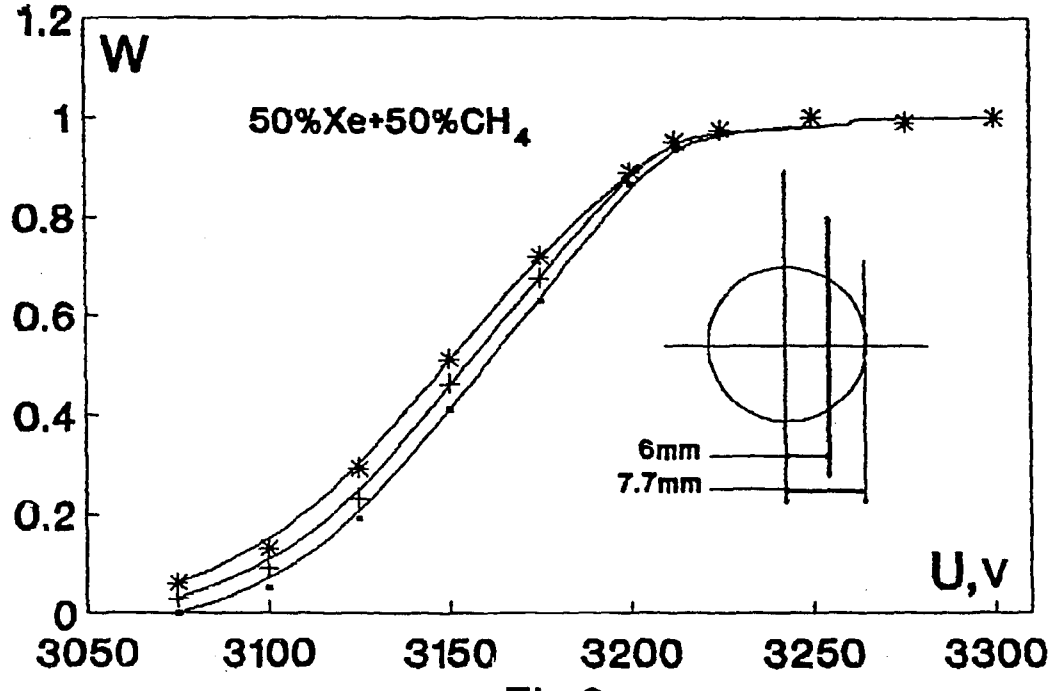
1.2
1
0.8
0.6
0.4
0.2
0
W
50%Xe+50%CH_4
6mm
7.7mm
U,v
3050
3100
3150
3200
3250
3300

Fig.8

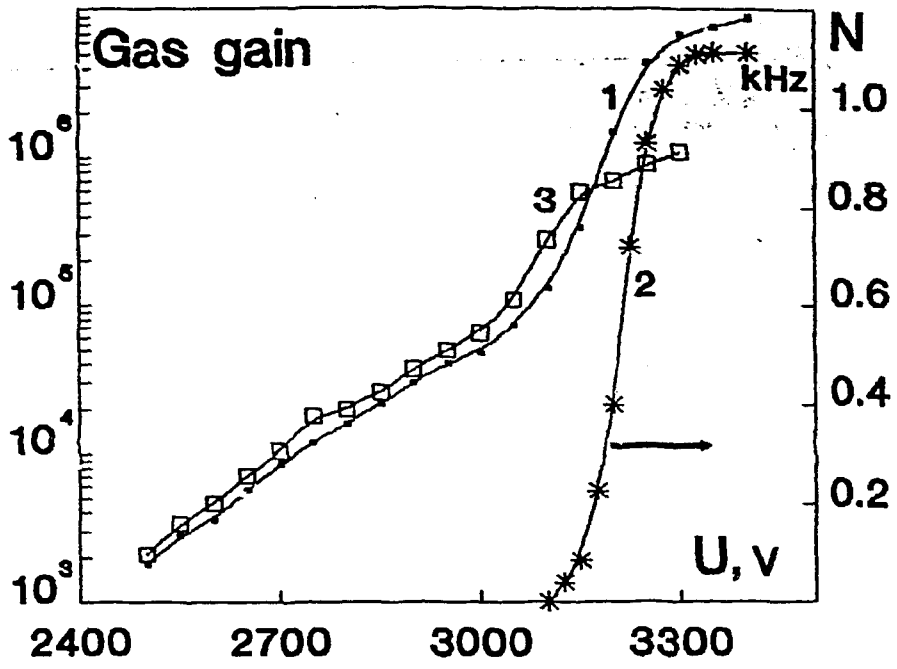
Gas gain
N
kHz
1
2
3
10^6
10^5
10^4
10^3
1.0
0.8
0.6
0.4
0.2
U, v
2400
2700
3000
3300

Fig.9

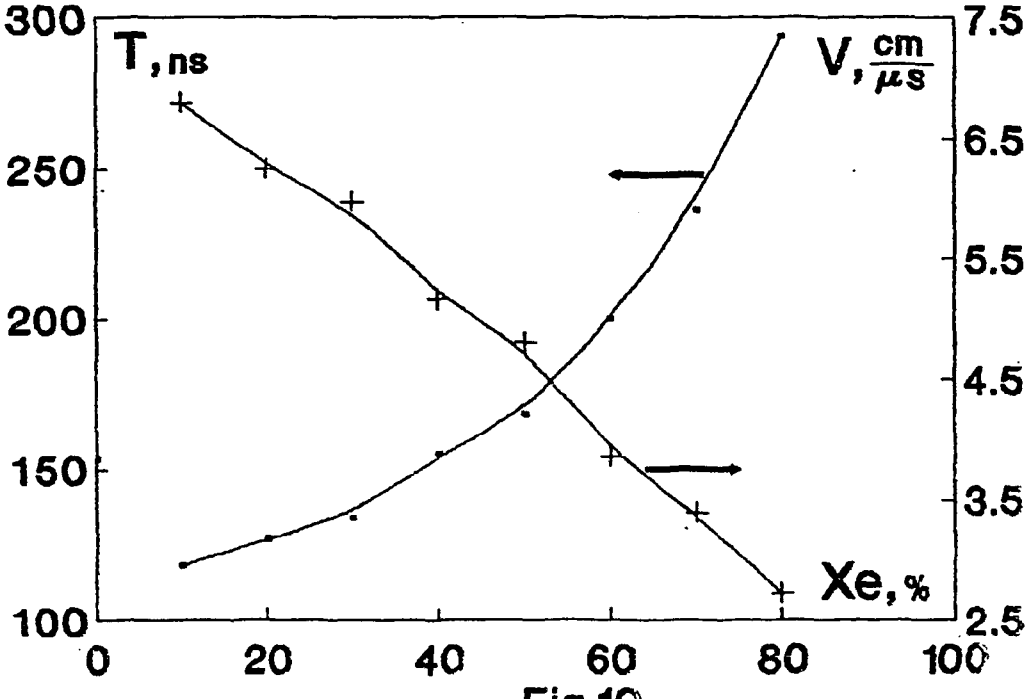
T, ns
V, $\frac{cm}{\mu s}$
Xe, %
300
250
200
150
100
7.5
6.5
5.5
4.5
3.5
2.5
0
20
40
60
80
100

Fig.10

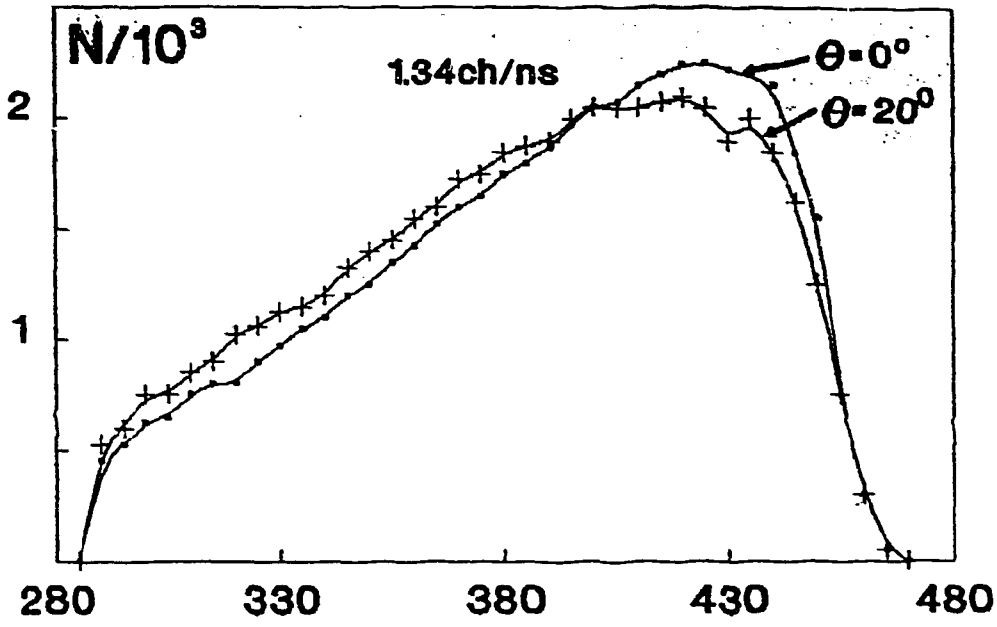
N/10³
1.34ch/ns
θ=0°
θ=20°
2
1
280
330
380
430
480
channels
Fig.11

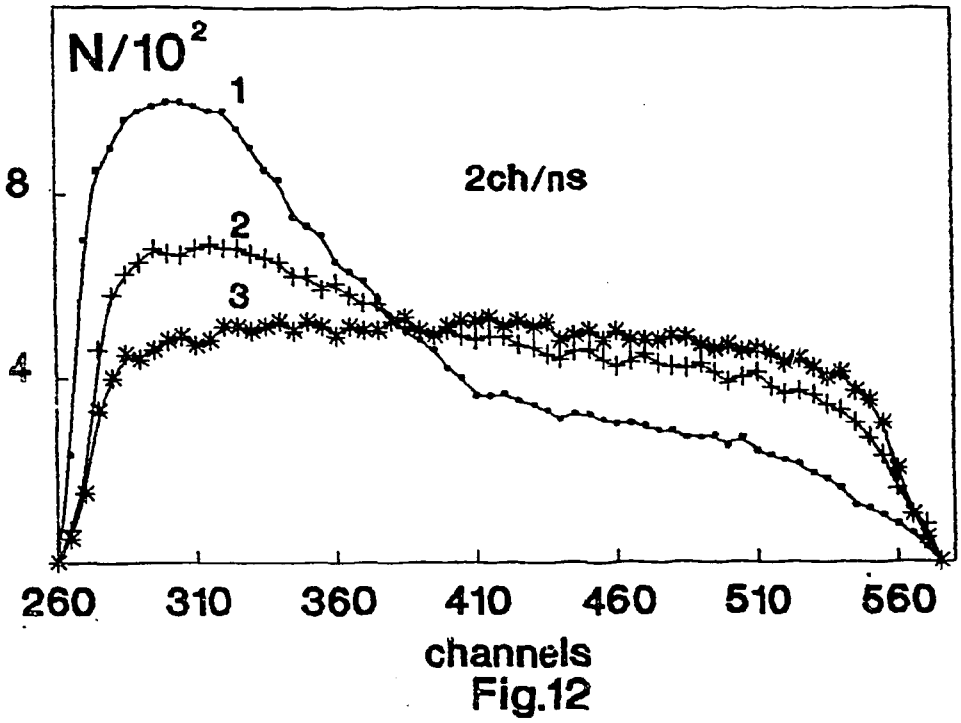
N/10²
1
2ch/ns
2
3
8
4
260
310
360
410
460
510
560
channels
Fig.12

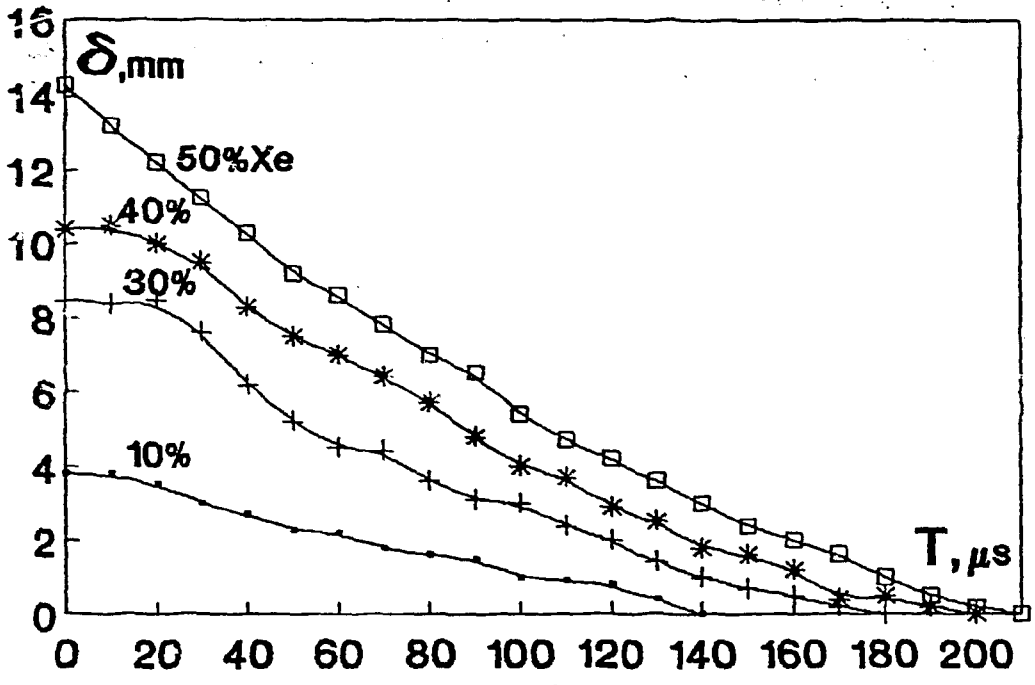
δ,mm
50%Xe
40%
30%
10%
T, μs
0
2
4
6
8
10
12
14
16
0 20 40 60 80 100 120 140 160 180 200
Fig.13

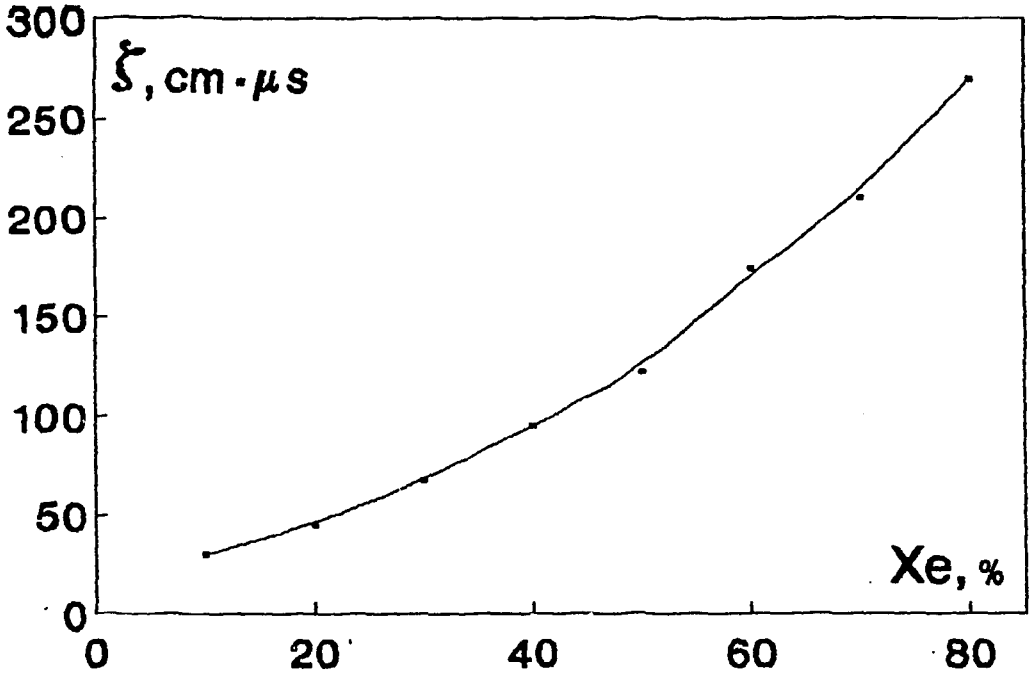
ζ, cm · μs
Xe, %
0
50
100
150
200
250
300
0 20 40 60 80
Fig.14

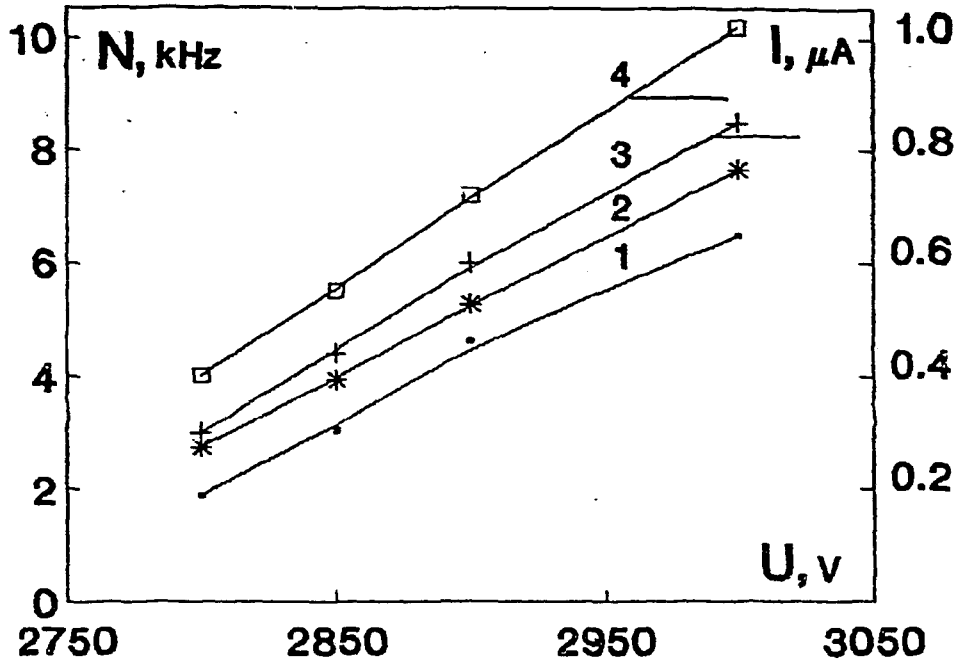
N, kHz
I, μA
U, V
10
8
6
4
2
0
1.0
0.8
0.6
0.4
0.2
2750
2850
2950
3050
1
2
3
4

Fig.15

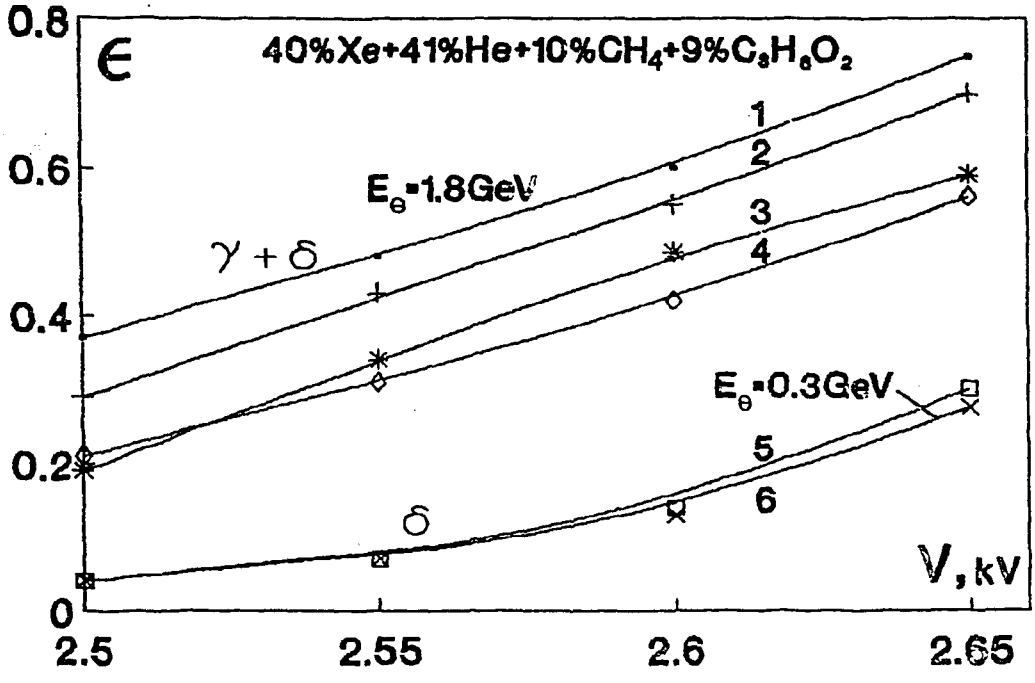
ϵ
40%Xe+41%He+10%CH4+9%C3H8O2
Eθ=1.8GeV
γ + δ
Eθ=0.3GeV
δ
V, kV
0.8
0.6
0.4
0.2
0
2.5
2.55
2.6
2.65
1
2
3
4
5
6

Fig.16

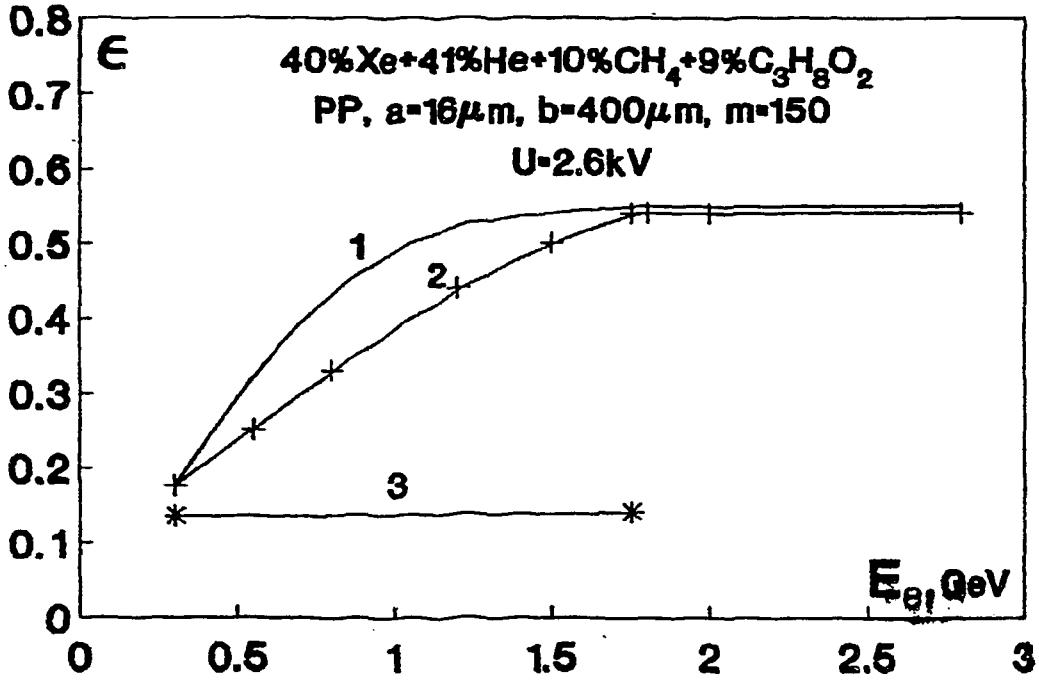
0.8
0.7
0.6
0.5
0.4
0.3
0.2
0.1
0
ϵ
40%Xe+41%He+10%CH4+9%C3H8O2
PP, a=16μm, b=400μm, m=150
U=2.6kV
1
2
3
Eel,GeV
0
0.5
1
1.5
2
2.5
3
Fig.17

Figure Captions

Fig.1 Two TRD configurations with an equal number of straws and amount of matter.

Fig.2 Monte Carlo calculation of the e/π-rejection factor as a function of electron detection efficiency in the mode of self-quenching streamer for the two TRD configurations shown in Fig.1 for x=5mm and x=8mm (see the text).

1. 24 single straw rows
2. 12 doubled straw rows

Fig.3 The view of the 12-module TRD model. On top - the electronics for 256 registration channels.

Fig.4 The spectra of the streamer signals from ^{55}Fe quanta and ^{90}Sr electrons. The quantum detection efficiency is 86%, the electron detection efficiency is 9%.

Fig.5 1-Rutherford distribution $P(E)\sim E^{-2}$ for δ-clusters with the given energy E:

2-curve of the probability of transformation into a streamer for the cluster of the given energy E;

3-the spectrum $W(E)=P(E)\cdot W_{str}$ of δ-clusters having transformed into streamer.

Fig.6 Spectral distributions of the streamer signals from ^{55}Fe and ^{241}Am quanta. The spectrum shift observed is 17%. cal- calibration curve.

Fig.7 The minimum ionizing electron detection efficiency as a function of Xe concentration in different gaseous mixtures:

a-$Xe+He+CH_4+C_3H_8O_2$. The probability of transformation of quanta with different energy into a streamer is given near the curves;

b-$Xe+CH_4$. The probability of transformation of ^{55}Fe quanta into a streamer is given near the curves.

Fig.8 The ^{55}Fe quanta detection efficiency as a function of the voltage applied and the location of straws bombardment.

Fig.9 GGF as a function of the voltage applied to the straws for two gaseous mixtures:

1-40%Xe+60%CH_4; 2-counting rate for 40%Xe+60%CH_4; 3-42%Xe+28%CH_4+30%$C_3H_8O_2$.

Fig.10 The total drift time and drift velocity as functions of Xe concentration in the gaseous mixture of $Xe+CH_4$.

Fig.11 Time spectra of clusters measured at U=3.2kV in straws with gaseous mixture of 50%Xe+50%CH_4, without collimation.

Fig.12 Time spectra of clusters initiated at U=3.15kV in straws with gaseous mixture of 50%Xe+50%CH_4 by electrons collimated onto the wire.

Fig.13 The "dead" length as a function of time at different Xe concentrations.

Fig.14 The "dead" zone ξ as a function of Xe concentration.

Fig.15 Noises in the SQS mode in case of 60Å aluminum coating. 1,3-without additional illumination; 2,4-with additional illumination.

Fig.16 The efficiency of electron detection in one straw as a function of supply voltage in case of different radiators:

1-PP, a=16μm, b=1500μm, m=150, E_e=1.8GeV 2-PP, a=16μm, b=400μm, m=150, E_e=1.8GeV

3-Polystyrene foam PS-4, ρ=0.04g/cm^3, E_e=1.8GeV

4-Polystyrene foam PS-10, ρ=0.1g/cm^3, E_e=1.8GeV

5,6-without radiator at E_e=0.3GeV and 1.8GeV.

Fig.17 Electron detection efficiency as a function of energy for one straw:

1 - over γ+δ clusters (theory);

2 - over γ+δ clusters (experiment);

3 - over δ-clusters (experiment).

References

1. V.A. Polychronakos et al, CERN/DRDC/90-39, (1990).

2. P. Astier et al. CERN-SPSLC/91-21, (1991).

3. R.O. Avakian et al. Proc. Third workshop "Physics at UNK", Protvino, September 25-28, (1990), 165.

4. R.E. Ajvazian et al. Proc. of the 2nd Symp. on High energy Particles Transition Radiation, Yerevan, September 13-15, (1983), 744.

5. R.S. Ajvazian et al. Proc. International Symposium on Instrumentation for Colliding Beam Physics Novosibirsk, (1984), 207.

6. K.K. Shikhliarov Author's certificate 1274546, 1984, published in BI 24, (1987), 271, Moscow.

7. Raether. " Electron Avalanches and Breakdown in Gases- Butterwiths, London, (1966).

9. F. Sauli, Preprint CERN 77-09, p.2.

8. Breskin et al. NIM, 143 (1977), 29.

10. P. Huber et al., Helv. Phys. Acta, 20 (1947), 525.

11. E.Pfunfer "Radiation Detectors" Translated from German, (1961), Moscow, 32.

12. G.D. Alekseev et al. Preprint JINR 13-80-545, (1980).

13. V.M. Aulchenko et al. Preprint INT 85-122, (1985), Novosibirsk.

14. S.V. Yerin Preprint HEPI 88-103, Serpukhov, (1988).

15. Yu.A. Budaghov et al. Preprint JINR P13-92-200, Dubna, (1992).

The manuscript was received October 14 1993

К.К.ШИХЛЯРОВ, В.Г.ГАВАЛЯН,М.А.АГИНЯН
РЕГИСТРИРУЮЩАЯ ЧАСТЬ ДЕТЕКТОРА РЕНТГЕНОВСКОГО ПЕРЕХОДНОГО ИЗЛУЧЕНИЯ ДЛЯ УСТАНОВКИ ГИНЕС
(на английском языке, перевод Папяна Г.А.)

Редактор А.С.Есин
Технический редактор А.С.Абрамян

Подписано в печать 4/XI-93г. Формат 60x84/16
Офсетная печать.Уч.изд.л.I.5 Тираж I00 экз.
Зак. тип.№I62 Индекс 3649

Отпечатано в Ереванском физическом институте
Ереван 36, ул.Братьев Алиханян,2

Նախնատիպ ԵրՖԻ- [illegible]

Կ.Կ.ՇԻԽԼՅԱՐՈՎ, Վ.Գ.ՂԱՎԱԼՅԱՆ, Մ.Ա.ԱՂԻՆՅԱՆ

ԱՆՑՈՒՄԱՅԻՆ ՃԱՌԱԳԱՅԹՄԱՆ ԴԵՏԵԿՏՈՐԻ ԳՐԱՆՑՈՂ ՄԱՍԸ ԳԻՆԵՍ ՍԱՐՔԱՎՈՐՄԱՆ ՀԱՄԱՐ

Աշխատանքում քննարկված է անցումային ճառագայթման դետեկտորի գրանցող մասը, հիմնված բարակպատ մայլարե խողովակների վրա։ Մանրակրկիտ ուսումնասիրված է քսենոնով լցված խողովակների աշխատանքը ինքնամարող ստրիմերի ռեժիմում։ Չափումները կատարված են ինչպես ռադիոակտիվ, այնպես էլ Երևանի էլեկտրոնային սինքրոտրոնի փնջի վրա։

Երևանի ֆիզիկայի ինստիտուտ

Երևան

ПРЕПРИНТ ЕФИ 1445 (15)-95

К. К. ШИХЛЯРОВ, В. Г. ГАВАЛЯН

РЕГИСТРИРУЮЩАЯ ЧАСТЬ ДЕТЕКТОРА РЕНТГЕНОВСКОГО ПЕРЕХОДНОГО ИЗЛУЧЕНИЯ ДЛЯ УСТАНОВКИ ГИНЕС

В работе рассматривается регистрирующая часть детектора рентгеновского переходного излучения, построенная на основе тонкостенных майларовых трубок. Подробно изучена работа трубок с ксеноновым наполнением в ре ме самогасящегося стримера. Измерения выполнены как с помо о радиоактивных источников. так и на пучке электронов Ереванскс синхротрона.

Ереванский физиче й институт

Ереван

Preprint YERPHI

Shikhliarov, V.G.Gavalian, M.A.Aginian

DETECTING PART OF TRD FOR GINES INSTALLATION

The detecting part of an X-ray transition radiation detector based on thin-walled mylar straws is considered in this paper. The performance of xenon-filled straws in the self-quenching mode is studied in details. The measurements have been carried out both with radioactive sources and under the electror beam of Yerevan synchrotron.

Yerevan Physics Institute
Yerevan